Available online at www.sciencedirect.com
SCIENCE DIRECT®
International Journal of Fatigue 25 (2003) 489–497
International Journal of Fatigue
www.elsevier.com/locate/ijfatigue

Molecular fatigue in steamed wood

Petri P. Kärenlampi *, Pekka Tynjälä, Pasi Ström

University of Joensuu, Faculty of Forestry, P.O. Box 111, FIN-80101 Joensuu, Finland

Received 30 May 2002; received in revised form 25 November 2002; accepted 29 November 2002

Abstract

Cyclical off-axis compression was applied to steamed Spruce wood in uniaxial strain under stress control. It has previously been shown that stiffness decrement and plastic strain due to mechanical fatigue loading are closely related, and both depend on the greatest accumulated strain. Molecular fatigue response was now investigated in terms of Differential Scanning Calorimetry. In accordance with classical Coffin-Manson theory, it was found that the creation of fatigue damage depends on plastic strain amplitude, not depending on the applied stress, applied strain, or the amount of dissipated energy as such. Molecular reorganization becomes more pronounced along with further energy application, as well as with increased process temperature.

Keywords: Cell wall porosity; Thermoporosimetry; Molecular fatigue; Strain level; Strain amplitude; Energy dissipation; *Picea Abies*

1. Introduction

Wood is an anisotropic composite of polymeric constituents. It is widely available, and used for a variety of purposes, including constructions, joinery, pulp and paper, as well as for fractionation into chemicals. A variety of such industries apply steam treatment as a process means, just to mention moisture and temperature softening of joinery components, as well as steaming of wood in the context of mechanical and chemical pulping. The mechanical properties of steam-treated wood are of interest in all those industries which combine steam treatment with mechanical action. Mechanical pulping processes essentially consist of fatigue treatments, intending to loosen the internal structure of steam-treated wood.

Wood is a rather complex composite of polymeric constituents. The different constituents, cellulose, hemicelluloses and lignins, have significantly different properties. In the abundance of water, hemicelluloses tend to soften below room temperature, where lignins and cellulose still remain stiff [1–5]. A widely accepted hypothesis is that the softening of lignins largely dominates the effect of temperature and moisture on time-dependent mechanical behavior of wood, at least in the range of moisture and temperature applicable in industrial steaming operations, between 100 and 200 °C, cellulose still remaining stiff in such temperatures [4,6].

Wood is a highly anisotropic composite. A tree bole is in coarse terms cylindrical, and displays rotational symmetry with respect to the central axis. The cellulose microfibrils are approximately aligned in the longitudinal direction. Mechanical stiffness is much higher in the direction of the cellulose microfibrils than in the transverse directions. The cellulose is less susceptible to thermal and moisture-induced softening than the surrounding matrix of hemicellulose and lignin, and thus increasing temperature and moisture in general increase mechanical anisotropy [1,2,3,7,8, cf. 9].

Stress–strain behavior of cellular materials in general is non-linear [10,11]. In particular, *radial* and *tangential* compression of wood first display an apparently linear elastic range, after which strain can be increased without any major increment of stress [12–17]. This 'plateau region' is likely to be due to buckling of cell walls into the cell lumens [12, 13,15,18, 19, cf. 20, 21]. Once the strain becomes so large that the space in the lumens available for cell wall buckling becomes limited, the compressive stress again starts to significantly increase as a function of increasing compressive strain [13–17]. Short-time mechanical behavior of wood may signifi-

* Corresponding author. Tel.: +358 13 251 4009; fax: +358 13 251 3590.
E-mail address: petri.karenlampi@joensuu.fi (P.P. Kärenlampi).

0142-1123/03/$ - see front matter © 2003 Elsevier Science Ltd. All rights reserved.
doi:10.1016/S0142-1123(02)00175-5

cantly depend on the degree of hydraulic filling of the cell lumens [10,15].

The stress–strain compression behavior of wood in the longitudinal direction has been observed to differ significantly from the stress–strain behavior in the transverse directions, the longitudinal direction showing instabilities at strains of a few percent, manifested as decrement of stress as a function of increasing strain [13,22]. Longitudinal instability appears to depend not only on stress but also on loading time, as well as the number of applied loading cycles [23,24].

Consisting of amorphous polymers, wood displays time-dependent mechanical behavior. However, at least up to 100 °C, 50% compressive engineering strain in the radial direction, and straining time of a few seconds, true irrecoverable (plastic) deformation in wood has been found to be small [15,16]. Thus, at least in radial compression, wood appears to behave viscoelastically. However, there is no definite reason to assume that the mechanical response would still be viscoelastic in other material directions, greater temperatures, and with longer straining times [cf. 22,25,26].

The mechanical behavior of steamed wood under cyclical compression has recently been investigated [27,28]. Investigations have shown that even though the mechanical behavior in terms of energy dissipation, strain amplitude and dynamic stiffness is rather sensitive to stress level and stress amplitude, the decrement of small-strain stiffness has been an almost unique function of the level of greatest compressive strain which has appeared during loading [28,29]. The stiffness decrement has been closely related to plastic strain [27–29]. Thus small-strain stiffness and plastic strain have not appeared to reflect the variety of material reactions to fatigue treatments.

In heterogeneous hydrated systems, the amount of water with depressed melting temperature is detectable using Differential Scanning Calorimetry (DSC) [30–33,35]. It is known that water in pores of nanometer scale does not freeze at all. This can be explained in a variety of ways. One of the simplest explanations is that in a space of size close to that of a molecule, there is not much room for molecular motion. Thus the matter appears solid-like, regardless of the temperature, and no thermal transition between solid and liquid is recognized [53]. Molecular mobility may also be reduced due to adsorption to sites like ionic groups [54–56]. Alternatively, one might explain the existence of non-freezing water in terms of slowness of diffusion at low temperature and in small capillaries [57].

The porosity of the wood fiber cell wall increases along with decreasing yield in the course of chemical pulping [34,36–38], and increases in the course of mechanical pulping and chemical pulp beating [34,37–39]. It has been recently shown that the cell wall porosity significantly evolves along with wood basic density, as a function of position within an annual ring, the non-freezing water content of fresh earlywood being less than the non-freezing water content of fresh latewood [40].

Considering the change in cell wall porosity along with pulping operations, it may be of interest to study how the cell wall porosity, and particularly the non-freezing water content of wood cell walls can possibly be changed through mechanical treatment by compression. Thus we will investigate dynamic mechanical behavior of spruce wood, steam-treated at 130 °C. In particular, we will explore the molecular response of specimens subjected to off-axis compressive fatigue loading in unidirectional strain. First, we will describe experimental arrangements. Then, we will report the evolution of compressive strain and dynamic stiffness the course of cyclic compressive loading, and address the energy dissipation during such loading. Finally, the effect of process variables on the changes in cell wall porosity in the nanometer scale will be reported.

2. Materials and methods

Spruce heartwood specimens of dimensions $34 \times 34 \times 9$ mm and of dry mass 4.0 g (±5%), frozen as fresh and then thawed in water overnight, were treated with saturated water steam at 130 °C. After steaming of 40 min, experiments were conducted by compressing any specimen in uniaxial strain in the direction of 9 mm thickness, which in turn was prepared in order to correspond to half way between the tangential and longitudinal material directions. In other words, specimens of 9 mm thickness were sawn along a plane at a 45° angle with respect to the longitudinal direction of the tree trunk, at a 45° angle with respect to the local tangent of the tree trunk cross-section, the specimen thickness being perpendicular to the local radius of the tree trunk. The location of off-axis specimens in a tree trunk is shown in Fig.1.

Off-axis compression was applied in order to experiment with a relatively simple arrangement which however induces a combination of stresses, including shear stresses, in the anisotropic material. Any specimen contained about 15 annual rings.

A previous investigation [29] has shown a stress–strain behavior for specimens of the present kind as shown in Fig. 2. Engineering stress as a function of logarithmic strain (‘true strain’) under monotonically increased compressive strain at rate 5%/s is shown for two specimens. After reaching 80% compressive strain, the strain was released under strain control, using the same strain rate. Along with monotonic straining at rate 5%/s, two instabilities are found, the instabilities roughly corresponding to 5% and 65% of compressive strain. Compressing once to 80% compressive strain has significantly changed the mechanical behavior as shown in Fig. 2.

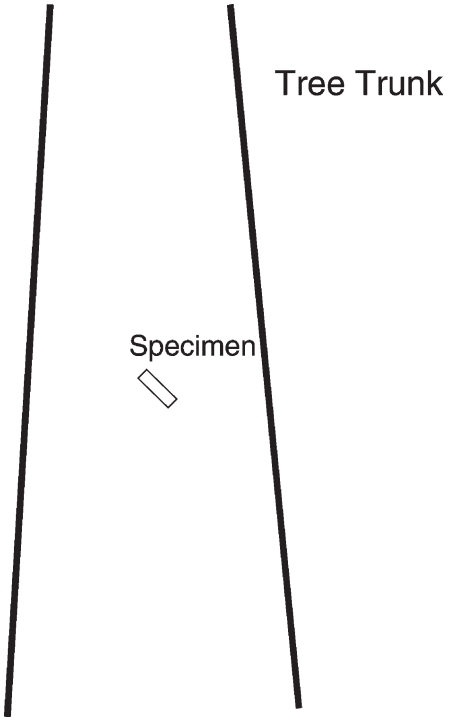

Fig. 1. The location of off-axis specimens in a tree trunk.

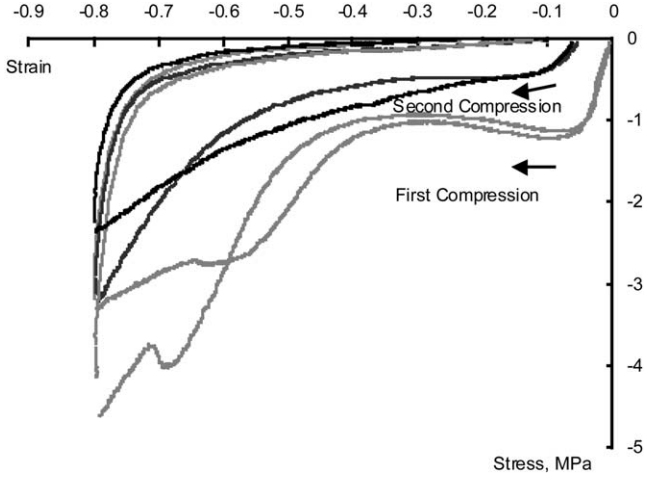

Fig. 2. Stress–strain behavior of two off-axis specimens in first and second compression at rate 5%/s.

Periodic tests were conducted by applying a sinusoidal stress of constant set point and amplitude, using a servohydraulic testing machine which was considered rather stiff in comparison to the stiffness of steamed wood. Fig. 2 was made using in the selection of the applied stress range. Some of the tests were conducted with a greatest compressive stress of 0.9 MPa, which does not induce instability of strain in short-term loading (Fig. 1). In order to experiment with greater stresses, peak compressive stresses of 2.7 and 6.0 MPa were used. All tests were conducted at 10 Hz loading frequency and intended energy application of 10 MJ/m^3, which practically led to test durations between 9 and 130 s. Forces due to inertia were negligible in these experiments.

Two levels of relative double amplitude of stress were used. The double amplitude in relation to peak compressive stress was taken as either 30% or 90%. In other words, either 30% or 90% of applied compressive stress was released within any loading cycle. Such arrangements correspond to stress ratios 1.43 and 10.0, the stress ratio taken as the peak compressive stress in relation to the minimum compressive stress. The periodic off-axis loading program, consisting of 12 specimens, is shown in Table 1. Table 1 also reports the amount of mechanical work applied to any specimen, as well as the amount of energy dissipated within any test; energy which did not recover within release of compressive strain was considered as dissipated.

Fig. 3 illustrates a typical periodic experiment. The stress is changed sinusoidally between 2.7 and 0.3 MPa at a frequency of 10 Hz, the strain evolving as the experiment proceeds.

After dynamic loading, an earlywood specimen of dry mass 5 mg was produced from any of the loaded specimens, using a sharp knife. Any small earlywood specimen, along with 10 mg of deionized water, was placed in a Differential Scanning Calorimeter within 15 min from the termination of dynamic loading, and frozen to −45 °C at rate 10 °C/min. Then, the temperature was increased to +25 °C at rate 5 °C/min, and the amount of melting water was determined through the measurement of melting enthalpy. The total amount of water within the specimen was determined through drying the specimen and deducting the dry mass from the total mass. The distinction between the total amount of water and the melting water was taken as the amount of non-freezing water (NFW). In accordance with the Gibbs–Thompson equation, it was assumed that water in pores which are small enough does not freeze at −45°C, and the amount of NFW within a specimen in relation to the dry mass of the specimen was taken as a measure of porosity in the nanometer scale.

3. Evolution of strain

The evolution of strain level within any test is shown in Fig. 4. Fig. 4 displays the greatest compressive (logarithmic) strain detected within any loading cycle. We find that the strain level is a function of the applied stress level.

Compressive stresses up to 0.9 MPa, of which 90% has been released within any loading cycle, appear to induce rather small compressive strains. The same peak stress does induce a significant strain when released to only 70% of the peak stress (30% relative double stress amplitude). It thus appears that the material approaches the first instability of strain, visible in Fig. 2, in a way

Table 1
The dynamic loading program

Peak compressive stress (MPa)	Double stress amplitude (MPa)	Loading frequency (Hz)	Number of cycles	Applied energy (MJ/m^3)	Dissipated energy (MJ/m^3)
0.90	0.26	10	1300	7.6	0.4
0.90	0.81	10	1000	12.8	3.4
0.90	0.80	10	900	14.8	4.9
2.7	0.81	10	590	6.7	1.4
2.7	0.81	10	590	7.4	1.8
2.7	2.4	10	120	13.2	5.7
2.6	2.4	10	120	12.2	5.5
2.7	2.4	10	120	9.6	4.5
2.7	2.4	10	140	6.1	2.8
6.0	5.4	10	90	7.6	3.4
6.0	5.4	10	130	10.7	4.2
6.0	5.4	10	130	9.8	3.6

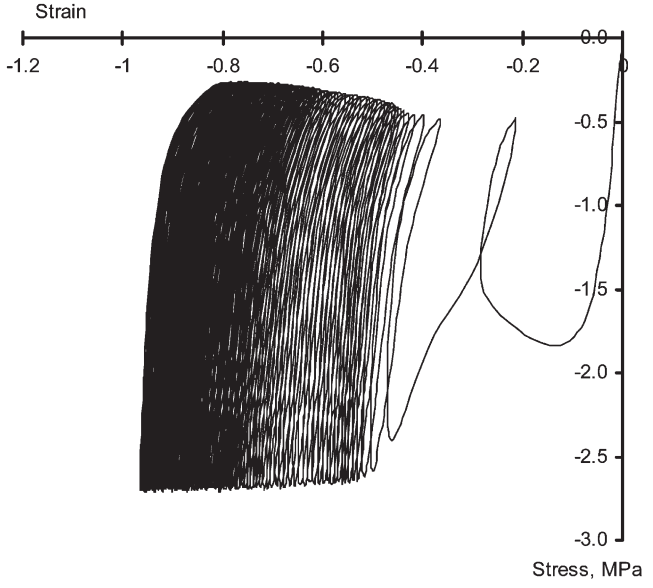

Fig. 3. Stress–strain behavior of a specimen in the course of a periodic experiment.

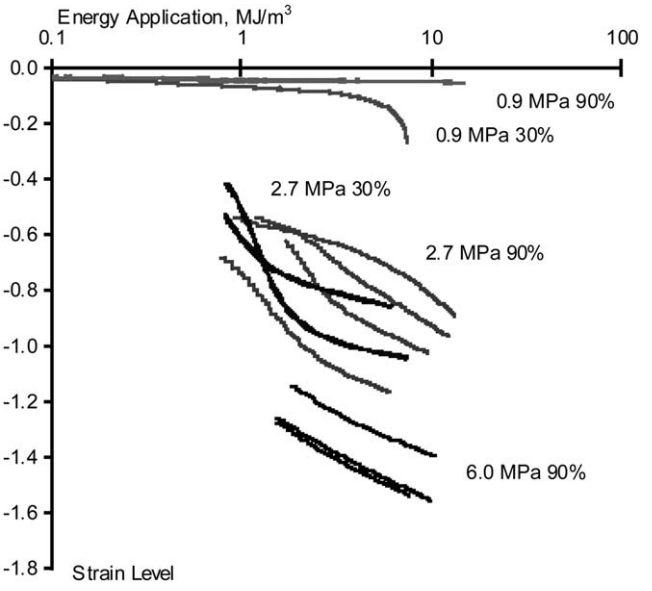

Fig. 4. Strain level as a function of energy applied per unit volume during dynamic loading. Curves are labeled according to greatest applied compressive stress level and relative double stress amplitude.

which depends either on load duration or the number of loading cycles, rather than stress amplitude or mechanical energy application.

Specimens loaded with peak compressive stress of 2.7 MPa already experience a significant compressive strain within the first loading cycle, after which the compressive strain level further evolves along with additional compression cycles (Fig. 4). Specimens loaded with 90% relative stress amplitude do not show significant saturation of the compressive strain increment, whereas the compressive strain increment rate within specimens loaded with 30% appears to decrease along with further loading.

4. Energy dissipation

The proportion of applied energy not mechanically recovered within three consecutive loading cycles is shown in Fig. 5. We find that the specimens loaded with 30% relative stress amplitude significantly differ from the specimens loaded with 90% relative stress amplitude. After energy dissipation in the context of the initial increment of compressive strain (cf. Fig. 4), the behavior of specimens loaded with the small relative amplitude is almost elastic, whereas 30–40% of the energy applied at 90% relative stress amplitude becomes dissipated, at all applied peak stress levels. It is somewhat remarkable that even specimens loaded with 0.9 MPa compressive

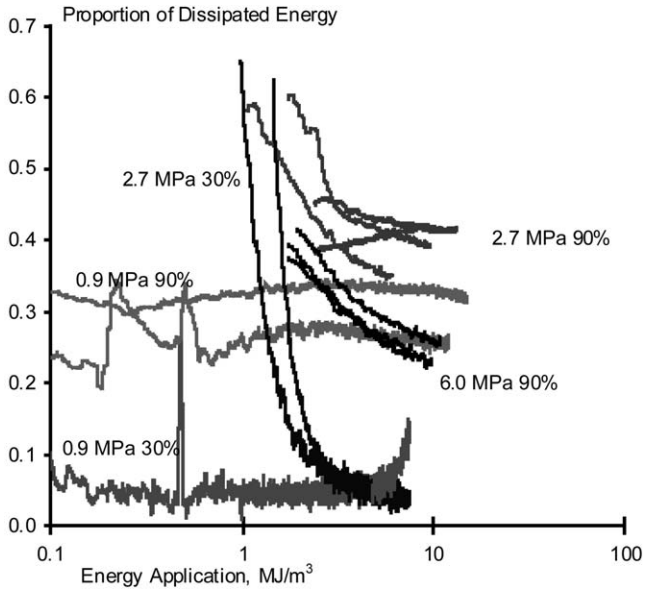

Fig. 5. Proportion of dissipated energy as a function of energy applied per unit volume during dynamic loading. Curves are labeled according to greatest applied compressive stress level and relative double amplitude of stress.

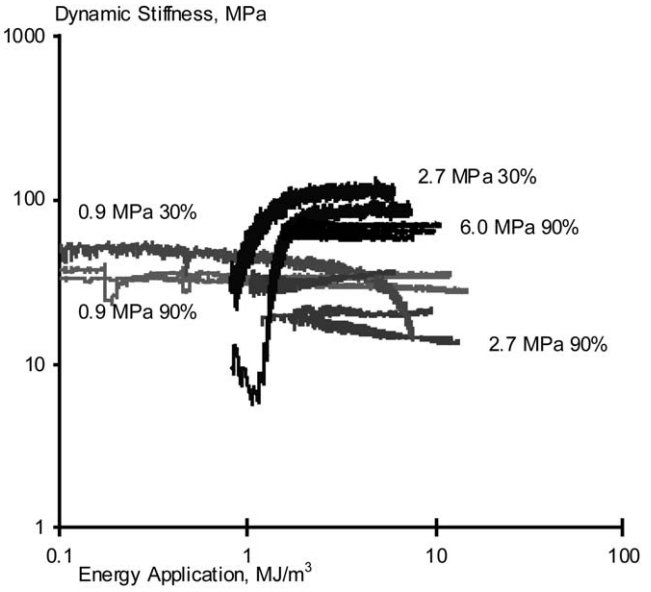

Fig. 6. Dynamic stiffness as a function of energy applied per unit volume in dynamic loading. Curves are labeled according to greatest applied compressive stress level and relative double amplitude of stress.

peak stress with 90% relative stress amplitude dissipate some 30% of the applied energy, even though the applied strain is rather small (cf. Fig. 4).

Fig. 5 further shows that in the case of at least 2.7 MPa peak stress and 90% relative stress amplitude, the energy dissipation rate decreases along with energy application. This may be associated with the increment of compressive strain level (cf. Fig. 4). With 6 MPa compressive peak stress, the proportion of dissipated energy is less than with 2.7 MPa compressive peak stress.

5. Dynamic stiffness

Dynamic stiffness, defined as the ratio of stress amplitude to strain amplitude during periodic loading, is shown as a function of energy application in Fig. 6. We find that specimens loaded with 30% relative stress amplitude show the greatest stiffness. Interestingly, specimens loaded with 2.7 MPa compressive peak stress and 90% relative stress amplitude show the lowest dynamic stiffness, specimens loaded with 0.9 MPa compressive peak stress showing a greater stiffness. Specimens loaded with 6 MPa compressive peak stress show much greater stiffness than specimens loaded with 2.7 MPa compressive peak stress.

We find from Fig. 6 that the dynamic stiffness hardly evolves during dynamic loading. There are two exceptions. The first exception is the initial increment of dynamic stiffness in the case of specimens loaded with 2.7 MPa peak stress and 30% relative stress amplitude. This increment of stiffness corresponds to the increment of strain level, shown in Fig. 4. The other exception from the invariance of stiffness during loading is the terminal decrement of stiffness of the specimen loaded with 0.9 MPa peak stress and 30% relative stress amplitude. This stiffness change corresponds to the instability of strain which the specimen approaches, as shown in Fig. 4.

6. Molecular fatigue

The non-freezing water content of moist, virgin spruce earlywood has been reported to be 16–20% of the dry mass of the wood [40]. Within the present investigation it was verified that the same applies to steam-treated earlywood in the absence of any mechanical fatigue loading. The non-freezing water content reflecting cell wall porosity in the nanometer scale, is here assumed to reflect microstructural damage due to mechanical treatment.

Previous investigations have shown that plastic strain, as well as decrement of small-strain stiffness modulus, due to mechanical compression fatigue treatment, is due to the greatest compressive strain which has appeared during loading, being insensitive to the details of the mechanical treatment [28,29]. However, the present results show that molecular fatigue, reflected in the non-freezing water content, is not dictated by the greatest strain applied during loading.

From Fig. 7 it is found that specimens being loaded with 2.7 MPa compressive peak stress and 30% relative double stress amplitude have experienced the same compressive strain as specimens loaded with 90% relative

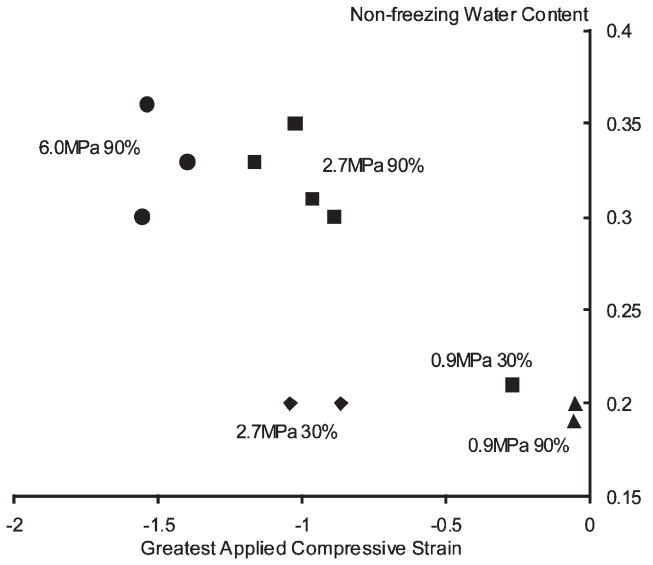

Fig. 7. Nanometer-scale porosity as a function of greatest applied compressive strain. Observations are labeled according to greatest applied compressive stress level and, relative double amplitude of stress.

double stress amplitude. The low-amplitude experiments however show only a very small increment in the non-freezing water content, whereas the molecular fatigue in specimens treated with the greater relative amplitude is rather pronounced.

Energy dissipation has been proposed as a measure of the efficiency of wood fatigue treatment [41,42]. However, we find from Fig. 8 that there does not appear to be much dependency between energy dissipation and porosity changes. In particular, specimens loaded up to 0.9 MPa compressive stress with 90% relative stress amplitude show the same level of energy dissipation as specimens loaded with greater compressive stresses, but they do not show any increment in non-freezing water content. Specimens loaded with 30% relative double stress amplitude show a small amount of dissipation and a small non-freezing water content, regardless of the applied stress level (Fig. 8).

Seminal observations regarding the thermal fatigue of metals have related the extent of fatigue damage to cyclical inelastic strain [43,45, cf. 45, 46]. Thus it appears reasonable to discuss inelastic strain amplitude as a fatigue process parameter. Fig. 9 shows the non-freezing water content as a function of the mean value of total double strain amplitude which occurred within any treatment.

It appears from Fig. 9 that the strain amplitude uniquely determines the magnitude of molecular reorganization. Within the present series of experiments, none of the specimens experiencing a double strain amplitude less than 5% shows a significant change in non-freezing water content. On the other hand, all specimens experiencing a double strain amplitude exceeding 5% do show a significant increment in non-freezing water content.

It is worth noting that specimens treated with 2.7 MPa peak compressive stress and 90% relative stress amplitude show a significant experimental scatter in the strain amplitude resulting from stress-controlled loading (Fig. 9). They also shown some scatter in the amount of energy dissipation (Fig. 8). However, there is much less scatter in the non-freezing water content.

It appears from Fig. 9 that the non-freezing water content would be discontinuous, the values being, at most, either 2.1 or at least 3. The authors however are not

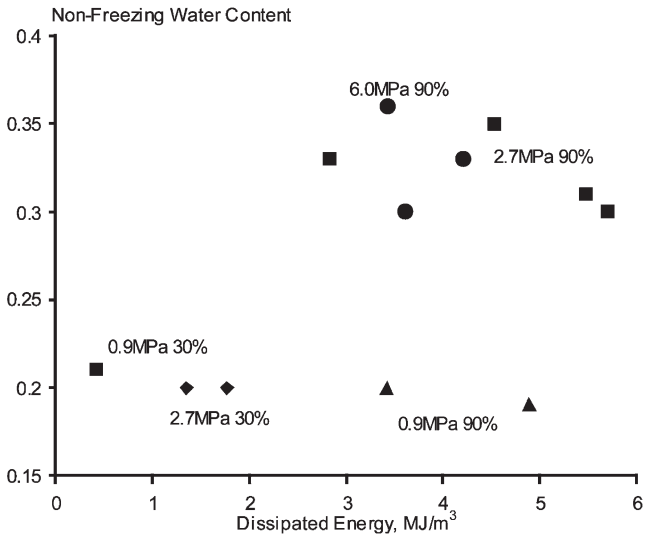

Fig. 8. Nanometer-scale porosity as a function of energy dissipated per unit volume. Observations are labeled according to greatest applied compressive stress level and relative double amplitude of stress.

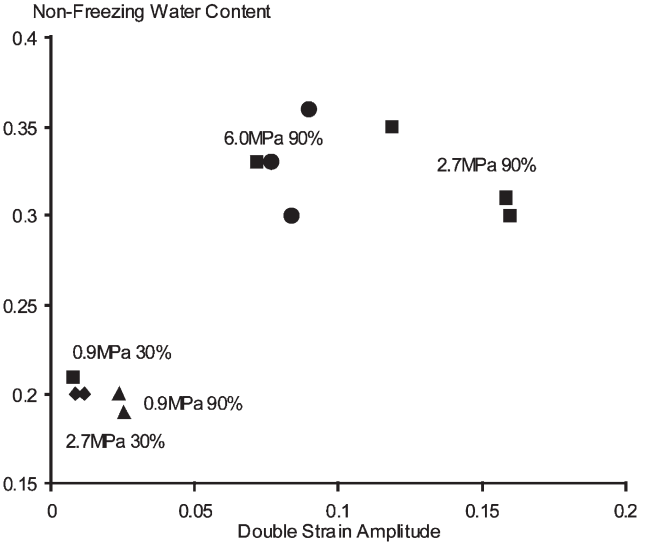

Fig. 9. Nanometer-scale porosity as a function of double strain amplitude. Observations are labeled according to greatest applied compressive stress level and relative double amplitude of stress.

aware of any mechanism inducing such discontinuity, and thus assume that it is only apparent.

7. Discussion

Previous investigations have shown that even though the mechanical behavior in terms of energy dissipation, strain amplitude and dynamic stiffness is rather sensitive to stress level and stress amplitude, the decrement of small-strain stiffness has been an almost unique function of the level of greatest compressive strain which has appeared during loading [28]. The stiffness decrement has been closely related to plastic strain [28,29]. Thus such measures have not appeared to reflect the variety of material reactions to fatigue treatments.

Nanometer-scale porosity does reflect the variety of material reactions to fatigue treatments. The extent of molecular reorganization appears to be related to strain amplitude (Fig. 9). It is, however, worth noting that in some particular treatments a double strain amplitude of 16% has resulted from stress-controlled loading, and this amount of strain amplitude has not induced more molecular reorganization than 8% double strain amplitude in some other cases (Fig. 9).

The seminal high-cycle fatigue approach [43, 44, cf. 45, 46] relates fatigue damage to cyclical *inelastic* strain. Cyclical *elastic* strain does not induce fatigue damage. Fig. 9 however shows the amount of molecular reorganization as a function of total strain amplitude. The practical reason for such a presentation is that the material behavior being highly nonlinear and very time-dependent, the elastic and inelastic strain amplitudes are difficult to separate. Anyway, it can be postulated that treatments involving greater stresses induce a greater amount of inelastic strain. Thus it is not difficult to understand that specimens loaded with compressive peak stresses of 6 MPa do show significant molecular reorganization even if the double strain amplitude does not exceed 10% (Fig. 9).

Even if significant molecular reorganizations took place during dynamic loading (Fig. 9), the dynamic stiffness, observed during the mechanical treatments, remained largely constant (Fig. 6). Thus it appears the molecular reorganization is not reflected in dynamic stiffness.

The invariance of stiffness along with loading, appearing in Fig. 6 is rather peculiar considering that the compressive strain level increases (Fig. 4). The increment of compressive strain level in the course of dynamic off-axis loading of a highly anisotropic composite may mostly be due to sliding shear deformation, not inducing major changes in the free volume contributing to mobility of molecules [cf. 47–51]. It is also possible that decrement of stiffness due to mechanical fatigue is to some degree compensated by somewhat reduced volume, resulting as a small net effect in dynamic stiffness.

Another peculiarity is that compressive strain accumulation is not straightforwardly time-dependent. The duration of experiments with 2.7 MPa compressive peak stress and 30% relative double stress amplitude was five times the duration of experiments with 90% relative double stress amplitude (Table 1), but the strain accumulation was no greater (Fig. 4). This is somewhat surprising since also the mean compressive stress within the 30% relative stress amplitude experiments was 55% greater than the mean compressive stress within the 90% relative stress amplitude experiments [cf. 23, 24].

A comparison of the extent of cell wall reorganization (Fig. 9) with the duration of any loading experiment (Table 1) shows that the molecular fatigue obviously does not depend on time under load. This is obvious since the duration of the experiments inducing significant molecular reorganization is between 9 and 14 s, these being the briefest experiments within the experimental program (Table 1).

It might be instructive to consider how the molecular reorganization possibly would be affected by a change in process temperature. In amorphous polymers, molecular mobility increases with increasing temperature [50–52]. Thus one can assume that decrement of temperature would reduce the rate of molecular reorganization.

The effect of temperature on molecular reorganization is shown in Fig. 10. We find that decrement of process temperature to 100 °C reduces the resulting non-freezing water content to 22%, the mechanical treatments being similar with 6 MPa peak compressive stress, 90% relative stress amplitude, 10 Hz loading frequency and 10 MJ/m^3 energy application per unit volume. Thus, 10

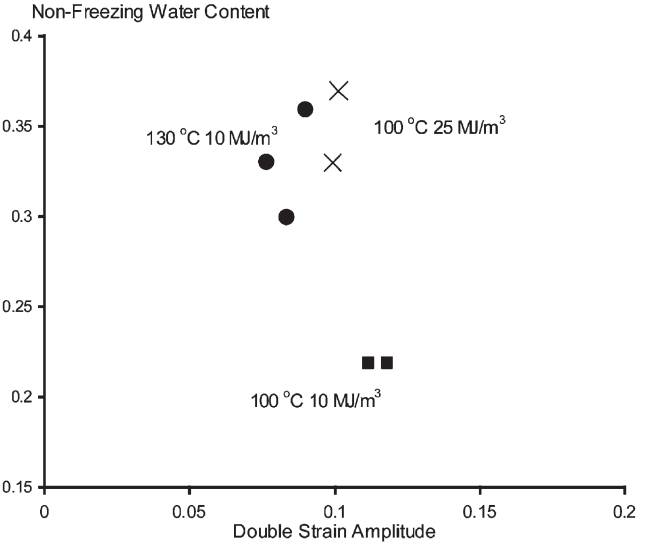

Fig. 10. Nanometer-scale porosity as a function of double strain amplitude, specimens being loaded with 6 MPa peak compressive stress, 90% relative double amplitude of stress, and 10 Hz loading frequency. Observations are labeled according to applied process temperature and amount of mechanical energy application per unit volume.

MJ/m^3 energy application only slightly increases nanometer-scale porosity.

In general, fatigue damage accumulates with the number of loading cycles [43, 44, cf. 45, 46]. Extending the treatment at 100 °C from 10 to 25 MJ/m^3 energy application per unit volume results in a molecular reaction which is at least at the same level as the result of the 10 MJ/m^3 energy application implemented at 130 °C (Fig. 10).

We further find from Fig. 10 that with constant stress amplitude, the strain amplitude is somewhat greater at the lower temperature.

It is worth noting that the molecular response to dynamic loading has here been discussed in terms of the non-freezing water content of 5 mg earlywood specimens. The non-freezing water content of latewood differs from that of earlywood, and the effect of some treatments is quite different [40]. The effect of dynamic loading on latewood remains to be investigated. It is still worth noting that not much is know at this stage regarding the exact physical mechanisms inducing the changes in cell wall structure, reflected in the changes in non-freezing water content.

Acknowledgements

The authors are obliged to the National Technology Agency of Finland for financing, and Dr Tomas Björkqvist for commenting on the manuscript.

References

[1] Kersavage PC. Moisture content effect on tensile properties of individual Douglas fir latewood tracheids. Wood Fiber 1973;5(2):105–17.
[2] Cousins WJ. Elasticity of isolated lignin: Young's modulus by a continuous indentation method. NZ J Forest Sci 1977;7(1):107–12.
[3] Cousins WJ. Young's modulus of hemicellulose as related to moisture content. Wood Sci Tech 1978;12:161–7.
[4] Salmén L. Viscoelastic properties of in situ lignin under water-saturated conditions. J Mater Sci 1984;19(9):3090–9036.
[5] Salmén L. Responses of paper properties to changes in moisture content and temperature. In: Tenth Fundamental Research Symposium, Oxford. Leatherhead (UK): Pira International; 1993. p. 369–430.
[6] Irvine GM. The significance of the glass transition of lignin in thermomechanical pulping. Wood Sci Tech 1985;19:139–49.
[7] Salmén L, Fellers C. The fundamentals of energy consumption during viscoelastic and plastic deformation of wood. International Mechanical Pulping Conference, EUCEPA, Oslo, 16–19 June, session VI, paper 1; 1981.
[8] Björkqvist T, Liukkonen S, Lucander M, Saharinen E. Kuidutuspinnan ja puun tehokkaampi vuorovaikutus (KUPU). Loppuraportti. Tampere University of Technology, Automation and Control Institute, report 4; 1998.
[9] Page DH, Schulgasser K. Evidence for a laminate model for paper. In: Mechanics of cellulosic and polymeric materials. New York: American Society of Mechanical Engineers; 1989. p. 35–9.
[10] Gibson LJ, Ashby JB. Cellular solids. Oxford: Pergamon Press; 1988.
[11] Christensen RM. Mechanics of cellular and other low-density materials. Int J Solids Struct 2000;37:104–33.
[12] Bodig J. The effect of anatomy on the initial stress–strain relationship in transverse compression. Forest Prod J 1965;15:197–202.
[13] Easterling KE, Harrysson R, Gibson LJ, Ashby MF. On the mechanics of balsa and other woods. Proc R Soc Lond A 1982;383:31–41.
[14] Grill J, Norimoto M. In: Birkinshaw C, Morlier P, Seoane I, editors. COST 508—wood mechanics, workshop on wood: plasticity and damage. CEC; 1993. p. 135–43.
[15] Uhmeier A. Some aspects on solid and fluid mechanics of wood in relation to mechanical pulping. Dissertation, Royal Institute of Technology, Stockholm; 1995.
[16] Uhmeier A, Salmén L. Influence of radial strain rate and temperature on the radial compression behavior of wet spruce. ASME JEMT 1996;118:289–94.
[17] Uhmeier A, Salmén L. Repeated large radial compression of heated spruce. Nordic Pulp Paper Res J 1996;11(3):171–6.
[18] March HW, Smith CB. Buckling loads of flat sandwich panels in compression. Various types of edge conditions. D.S.D.A. Forest Service, Forest Prods. Lab., Madison, Wis., report 1525, March 1945.
[19] Kunesh RH. Strength and elastic properties of wood in transverse compression. Forest Prod J 1967;18(1):65–72.
[20] Bienfait JL. Relation of the manner of failure to the structure of wood under compression parallel to the grain. J Agric Rec 1926;33(2):183–94.
[21] Kitahara R, Tsutsumi J, Matsumoto T. Observations on the cell wall response and mechanical behavior in wood subjected to repeated static bending load. Mokuzai Gakkaishi 1981;27(1):1–7.
[22] Kärenlampi PP, Tynjälä P, Ström P. Mechanical behavior of steam-treated spruce wood under compressive strain. Submitted for publication.
[23] Bach L. Frequency-dependent fracture in wood under pulsating loading. Forest Products Research Society Annual Meeting 1975, June 15, Portland, OR (The Technical University of Denmark, Department of Civil Engineering, Building Materials Laboratory, technical report 68/79); 1979.
[24] Clorius CO, Pedersen MU, Hoffmeyer P, Damkilde L. Compressive fatigue in wood. Wood Sci Tech 2000;34:21–37.
[25] Keith CT. The mechanical behavior of wood in longitudinal compression. Wood Sci 1972;4(4):234–44.
[26] Kärenlampi PP. Viscoplasticity of steam-treated wood. Submitted for publication.
[27] Kärenlampi PP, Tynjälä P, Ström P. Dynamic mechanical behavior of steam-treated wood. Mech Mater 2002;34(6):333–47.
[28] Kärenlampi PP, Tynjälä P, Ström P. Off-axis fatigue loading of steamed wood. Int J Fatigue 2002;24(12):1235–42.
[29] Kärenlampi PP, Tynjälä P, Ström P. The effect of temperature and compression on the mechanical behavior of steam-treated wood. J Wood Sci 2003; 49.
[30] Rennie GK, Clifford J. Melting of ice in porous solids. J Chem Soc F1 1977;73(4):680–9.
[31] Homshaw LG. Calorimetric determination of porosity and pore size distribution (PSD): effect of heat on porosity, pore form and PSD in water-saturated polyacrylonitrile fibers. J Colloid Interface Sci. 1981;84(7):127–40.
[32] Ishikiriyama K, Todoki M. Pore size distribution measurements of silica gels by means of differential scanning calorimetry. J Colloid Interface Sci 1995;171(1):103–11.
[33] Maloney TC, Paulapuro H, Stenius P. Hydration and swelling of

pulp fibres measured with differential scanning calorimetry. Nordic Pulp Paper Res J 1998;13(1):31–6.
[34] Maloney TC, Paulapuro H. The formation of pores in the cell wall. J Pulp Paper Sci 1999;25(12):430–6.
[35] Maloney TC. Thermoporosimetry by isothermal step melting. In: Proc. Pre-symp. of the 10th ISWPC, Seoul; 1999. p. 245–53.
[36] Stone JE, Scallan AM. The effect of component removal upon the porous structure of the cell wall of wood. II. Swelling in water and the fiber saturation point. Tappi 1967;50(10):496–501.
[37] Stone JE, Scallan AM, Abrahamson B. Influence of beating on the cell wall swelling and internal fibrillation. Sv Papperstidning 1968;71(19):687–94.
[38] Scallan AM. The accommodation of water within pulp fibers. In: 6th Fundamental Research Symposium 1977 (fiber-water interactions in papermaking). London; 1978. p. 9–29.
[39] Salmén LT, Tigerström A, Fellers C. Fatigue of wood-characterization of mechanical defibration. J Pulp Paper Sci 1985;11(3):68–73.
[40] Tynjälä P, Kärenlampi PP. Spruce cell wall porosity—variation within annual ring and drying response. First International Conference of the European Society of Wood Mechanics, 19–21 April, Lausanne, Swizerland; 2001. p. 39–45.
[41] Höglund H, Sohlin U, Tistad G. Physical properties of wood in relation to chip refining. Tappi 1976;59(6):144–7.
[42] Becker H, Höglund H, Tistad G. Frequency and temperature in chip refining. Pap Puu 1977;59(3):123–30.
[43] Coffin LFA. study on the effect of cyclic thermal stresses on a ductile metal. Trans Am Soc Mech Eng 1954;76:931–50.
[44] Manson SS. Behavior of materials under conditions of thermal stress. National Advisory Commission on Aeronautics: report 1170. Lewis Flight Propulsion Laboratory, Cleveland, OH; 1954.
[45] Suresh S. Fatique of materials, 2nd ed. Cambridge: Cambridge University Press; 1998.
[46] Kärenlampi PP. The effect of material disorder on fatigue damage induced by unidirectional loading. In: Gualgliano M, Aliabadi MH, editors. Advances in Fracture and Damage Mechanics II, Milan, Italy, 18–20 September. 2001. p. 87–92.
[47] Doolittle AK. Studies in Newtonian flow. II. The dependence of the viscosity of liquids on free space. J Appl Phys 1951;22(12):1471–5.
[48] Doolittle AK, Doolittle DB. Studies in Newtonian flow. V. Further verification of the free-space viscosity equation. J Appl Phys 1957;28:901–5.
[49] Ferry JD, Stratton RA. The free volume interpretation of viscosities and viscoelastic relaxation times on concentration, pressure, and tensile strain. Kolloid Zeitschrift 1960;171(2):107–11.
[50] Ferry JD. Viscoelastic properties of polymers. New York: John Wiley & Sons; 1961.
[51] Smith TLS. Stress–strain–time–temperature relationship for polymers. In: ASTM Materials Sci Series 3, STP-325. New York: ASTM; 1962. p. 60–89.
[52] Williams MI, Landel RF, Ferry JD. Temperature dependence of relaxation mechanisms in amorphous polymers and other glass-forming liquids. J Am Chem Soc 1955;77:3701–7.
[53] Berlin E, Kliman PG, Pallansch MJ. Changes in state of water in proteinaceous systems. J Colloid Interface Sci 1970;34(4):488–94.
[54] Berthold J, Despières J, Rinaudo M, Salmén L. Types of absorbed water in relation to the ionic groups and their counter-ions for some cellulose derivatives. Polymer 1994;35(26):5729–36.
[55] Berthold J, Rinaudo M, Salmén L. Associaton of water to polar groups; estimations by an adsorption model for lignocellulosic materials. In: 8th Int. Symp. Wood and Pulping Chemistry, Helsinki, Finland, 6–9 June. 1995. p. 575–80.
[56] Salmén L, Berthold J. The swelling ability of pulp fibers. In: 11th Fundamental Research Symposium, Cambridge, UK, 21–26 Sept. 1997. p. 683–701.
[57] Plouchly J, Biros J, Benes S. Heat capacities of water swollen hydrophilic polymers above and below 0 °C. Macromol Chem 1979;180(3):745–60.